

MATHEMATICAL MODELING OF SUSPENDED SEDIMENT IN NONUNIFORM FLOWS

By Leo C. van Rijn¹

ABSTRACT: A two-dimensional vertical mathematical model for suspended sediment is presented. The model is based on the width-integrated convection-diffusion equation for the sediment particles including settling effects. The local fluid velocities and mixing coefficients are described by a new so-called Profile model, which is based on the application of flexible profiles to represent the vertical distribution of the basic variables. Measured and computed velocities of strongly nonuniform flows were used for calibration of the Profile model. A stochastic approach is introduced to represent the sediment input at the bed. A bed concentration or an upward sediment flux can be specified (optional). The convection-diffusion equation is solved by a finite-element method, which proved to be better than a finite-difference method. An extensive sensitivity analysis is presented to show the influence of the main controlling parameters of the model. Finally, a verification analysis is presented using flume and field data of dredged trenches.

INTRODUCTION

A fundamental phenomenon of morphological processes is the continuous adjustment of the sediment transport to the sediment transport capacity, especially in environments with a predominant suspended load. The morphological processes in such conditions can be simulated sufficiently accurately by a simple one-dimensional flow model in combination with a sediment transport formula provided that the adjustment length is smaller than the grid size of the applied model. If this latter condition is not satisfied, the adjustment process should be modeled also.

In this paper, a two-dimensional (vertical) mathematical model is presented that represents the adjustment of the suspended sediment transport in detail.

Practical problems that may benefit from the use of such a model are the sedimentation in dredged channels and trenches, the sedimentation in reservoirs and basins, and the generation of scour holes.

Kerssens, Prins, and Van Rijn (8) presented a two-dimensional suspended sediment model for gradually varying flows. At that stage the vertical convection by the fluid was neglected. Simple logarithmic velocity profiles were used to represent the velocity field. A new expression for the sediment mixing coefficient was also introduced. At the bed boundary a concentration type of boundary condition was used, assuming direct adjustment of the near-bed concentrations to their equilibrium values. The bed concentration was computed from a total load formula. To solve the convection-diffusion equation a (six-point implicit) finite-difference method was used with a grid refinement towards the bed.

Van Rijn (11) extended the model to steep-sided channels and trenches by improving the computation of the velocity field (SUTRENCH model).

¹Sr. Engr., Delft Hydr. Lab., P.O. Box 152, Emmeloord, The Netherlands.

Note.—Discussion open until November 1, 1986. To extend the closing date one month, a written request must be filed with the ASCE Manager of Journals. The manuscript for this paper was submitted for review and possible publication on February 6, 1985. This paper is part of the *Journal of Hydraulic Engineering*, Vol. 112, No. 6, June, 1986. ©ASCE, ISSN 0733-9429/86/0006-0433/\$01.00. Paper No. 20652.

A fully empirical approach based on flume data was used. Reasonable results were obtained. However, the finite-difference solution method appeared to be unfavorable because relatively small space and time steps were required to obtain stable and accurate results. Therefore, it was decided to improve the suspended sediment model (SUTRENCH model) using a finite-element method. The flow width was introduced to describe the sediment transport in laterally varying flows. A new semi-empirical method has been developed to compute the longitudinal and vertical velocities and the mixing coefficients. This new method, which is called the Profile model, is based on the application of flexible profiles as suggested by Coles (3). To justify this new method, it has been compared with the sophisticated K- ϵ model (1,10) showing satisfactory results.

New stochastic functions for the bed-boundary condition were also developed and implemented. At choice (input parameter) the bed concentration or the upward sediment flux at the bed can be specified at each location as a function of local flow variables (bed-shear stress) and sediment size. These functions are based on theoretical and experimental research (16,17). The present paper describes the basic equations, simplifications, boundary conditions and numerical solution method of the suspended model, which is the standard model of the Delft Hydraulics Laboratory for suspended sediment predictions. A sensitivity analysis is presented to identify the main controlling parameters. Finally, a verification analysis is given using flume and field data.

BASIC EQUATIONS AND SIMPLIFICATIONS

The suspended sediment concentrations can be computed from the mass-balance equation, which reads for time-averaged variables in the vertical (x - z) plane, as follows (18):

$$\frac{\partial c}{\partial t} + \frac{\partial}{\partial x}(uc) - \frac{\partial}{\partial x}\left(\epsilon_s \frac{\partial c}{\partial x}\right) + \frac{\partial}{\partial z}(w - w_s)c - \frac{\partial}{\partial z}\left(\epsilon_s \frac{\partial c}{\partial z}\right) = 0 \dots\dots\dots (1)$$

in which c = local sediment concentration; u = local flow velocity in longitudinal (x) direction; w = local flow velocity in vertical (z) direction; w_s = particle fall velocity; ϵ_s = sediment mixing coefficient; and t = time. A definition sketch is given in Fig. 1.

Assuming steady-state conditions and neglecting the longitudinal diffusive transport, which usually is an order of magnitude smaller than the other terms (8), Eq. 1 reduces to

$$\frac{\partial}{\partial x}(uc) + \frac{\partial}{\partial z}(w - w_s)c - \frac{\partial}{\partial z}\left(\epsilon_s \frac{\partial c}{\partial z}\right) = 0 \dots\dots\dots (2)$$

Assuming the variables to be constant in lateral (y) direction, the sediment concentrations can be represented by integrating Eq. 2 over the (lateral) width of the flow, yielding

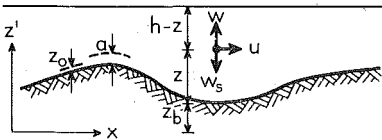


FIG. 1.—Definition Sketch

$$\frac{\partial}{\partial x}(buc) + \frac{\partial}{\partial z}b(w - w_s)c - \frac{\partial}{\partial z}\left(b\epsilon_s\frac{\partial c}{\partial z}\right) = 0 \dots\dots\dots (3)$$

in which b = width of the flow.

Eq. 3, which is the basic equation of the SUTRENCH model, can be solved numerically when the flow velocities (u, w), the sediment mixing coefficient (ϵ_s), the particle fall velocity (w_s), the flow width (b) are known and appropriate boundary conditions are specified.

FLOW VELOCITY PROFILES

Mathematical Models.—Various models can be applied to compute the velocity profiles in the x - z plane, depending on the degree of perturbation of the flow (large or small bed-level gradients).

For complicated flows with largely perturbed velocity profiles including flows with separation and reversal phenomena, a refined mathematical approach is of importance. The most accurate description of the velocity profiles can be obtained by applying the full Reynolds' equations for the fluid in combination with a two-equation (K - ϵ model) turbulence closure. The K - ϵ model, which is the most widely used model for complicated flows, consists of transport equations for the turbulence kinetic energy (K) and its dissipation rate (ϵ). Basic information of K - ϵ models has been summarized by Rodi (10). The applicability of the K - ϵ model for the computation of velocity profiles in trenches situated perpendicular to the flow has been reported by Alfrink and Van Rijn (1).

For routine long-term morphological computations implying the successive computation of the flow field, the K - ϵ model is not attractive because of excessive computer costs. To reduce the computation costs significantly, a new (simple) model has been developed which is based on flexible profiles as suggested by Coles (3) and simple first order differential equations. A fundamental drawback of the so-called Profile method is the need for experimental data over a wide range of conditions to calibrate the coefficients. When calibrated properly, the Profile method can be a powerful method for engineering practice.

Profile Model.—Coles (3) showed that the velocity profiles in a non-uniform flow can be described by using a linear combination of a logarithmic profile representing the law of the wall and a perturbation profile representing the influence of pressure gradients. In the present analysis a similar approach is used. The profile-model for the fluid velocities will now be described.

Longitudinal Velocity.—The velocity profile is described by

$$u = A_1 u_h \ln\left(\frac{z}{z_0}\right) + A_2 u_h F\left(\frac{z}{h}\right) \dots\dots\dots (4)$$

in which u = flow velocity at height z above bed; u_h = flow velocity at water surface ($z = h$); z_0 = zero-velocity level ($z_0 = 0.03 k_s$); k_s = effective roughness height; h = water depth; A_1 and A_2 = dimensionless variables.

The perturbation profile $F(z/h)$ is represented by

$$F\left(\frac{z}{h}\right) = 2\left[\frac{z - z_0}{h - z_0}\right]^t - \left[\frac{z - z_0}{h - z_0}\right]^{2t} \dots\dots\dots (5)$$

in which t = coefficient.

The A_2 variable can be determined by applying the boundary condition: $u = u_h$ for $z = h$ resulting in

$$A_2 = 1 - A_1 \ln \left(\frac{h}{z_0} \right) \dots \dots \dots (6)$$

Substitution of Eqs. 5 and 6 in Eq. 4 yields

$$u = A_1 u_h \ln \left(\frac{z}{z_0} \right) + u_h \left[1 - A_1 \ln \left(\frac{h}{z_0} \right) \right] \left[2 \left(\frac{z - z_0}{h - z_0} \right)^t - \left(\frac{z - z_0}{h - z_0} \right)^{2t} \right] \dots \dots (7)$$

The velocity profile, as described by Eq. 7, is completely defined when the unknown variables (A_1 , t , and u_h) are specified. Therefore, three additional equations must be specified, which are: (1) Equation of continuity; (2) equation for the t parameter; and (3) equation for the water-surface velocity, u_h .

Continuity Equation.—The discharge Q can be represented by

$$Q = b \int_{z_0}^h u \, dz \dots \dots \dots (8)$$

Substitution of Eq. 7 in Eq. 8 and integration yields

$$Q = \left[-1 + \ln \left(\frac{h}{z_0} \right) \right] A_1 b h u_h + \left[1 - A_1 \ln \left(\frac{h}{z_0} \right) \right] \left[\frac{3t + 1}{2t^2 + 3t + 1} \right] b h u_h \dots (9)$$

t Parameter Equation.—Analysis of velocity profiles measured in trenches situated perpendicular to the flow direction (4) showed that the measured mid-depth velocity at each location can be approximated by the mid-depth velocity computed from a logarithmic velocity profile at that location. The mid-depth velocity computed from the logarithmic velocity distribution is called the equilibrium mid-depth velocity. Thus

$$u_{\text{mid-depth}} = u_{\text{mid-depth, equilibrium}} \dots \dots \dots (10)$$

The mid-depth velocity according to Eq. 7 (for $z = 0.5 h$) is

$$u_m = A_1 u_h \ln \left(\frac{0.5 h}{z_0} \right) + u_h \left[1 - A_1 \ln \left(\frac{h}{z_0} \right) \right] [2(0.5)^t - (0.5)^{2t}] \dots \dots \dots (11)$$

The equilibrium mid-depth velocity, $u_{m,e}$, using a logarithmic velocity distribution can be described by

$$u_{m,e} = \frac{\ln \left(\frac{0.5 h}{z_0} \right)}{\left[-1 + \ln \left(\frac{h}{z_0} \right) \right]} \frac{Q}{bh} \dots \dots \dots (12)$$

Substitution of Eqs. 11 and 12 in Eq. 10 yields the t parameter equation

$$\left[\frac{-1 + \ln \left(\frac{h}{z_0} \right)}{\ln \left(\frac{0.5 h}{z_0} \right)} \right] = \frac{3t + 1}{[2t^2 + 3t + 1][2(0.5)^t - (0.5)^{2t}]} \\ \approx 0.16t^2 - 0.29t + 1.02 \dots \dots \dots (13)$$

Water Surface Velocity Equation.—The spatial variation of the velocity at the water surface is described by a simple first order differential

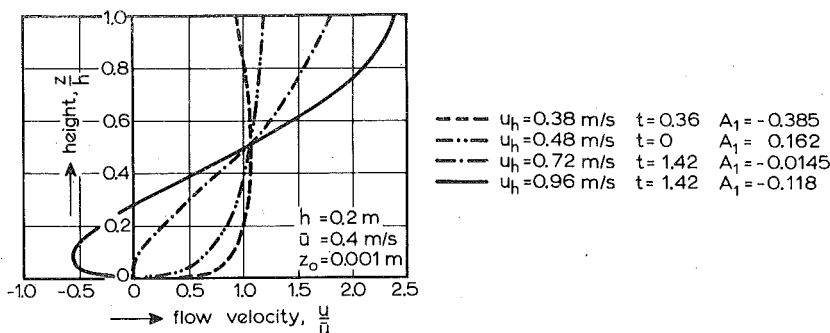


FIG. 2.—Velocity Profiles

equation, which yields an exponential adjustment of the surface velocity to the equilibrium surface velocity, $u_{h,e}$, as follows:

$$\frac{du_h}{dx} = \alpha_1 \frac{u_{h,e}}{h} - \alpha_2 \frac{u_h}{h} - \alpha_3 \frac{u_h}{b} \dots \dots \dots (14)$$

in which α_1 , α_2 , and α_3 = empirical coefficients to be determined by computer calibration using measured velocity profiles. The equilibrium surface velocity is defined as the surface velocity from a logarithmic velocity distribution. Eq. 14 can be solved numerically by using a simple Runge-Kutta method. The surface velocity at the inlet, $u_{h,0}$, must be known.

Fig. 2 shows some velocity profiles based on Eqs. 7, 9, and 13 for a given Q , b , h , and u_h . As can be observed, the Profile method is capable of representing a wide range of velocity profiles including those with flow reversal.

Vertical Flow Velocity.—The vertical flow velocity, w , can be computed from the width-integrated equation of continuity:

$$\frac{1}{b} \frac{\partial}{\partial x} (bu) + \frac{\partial}{\partial z} (w) = 0 \dots \dots \dots (15)$$

$$\text{yielding } w = - \int_{z_b+z_0}^{z_b+z} \frac{\partial u}{\partial x} dz - \frac{1}{b} \frac{db}{dx} \int_{z_b+z_0}^{z_b+z} u dz \dots \dots \dots (16)$$

Substitution of Eq. 7 in Eq. 16 and integration yields a (complicated) analytical expression (18).

Bed-Shear Velocity.—The local bed-shear velocity, u_* , which is needed to determine the bed-boundary condition for the sediment concentrations, is computed from the flow velocity at height $z = 0.05h$ above the mean bed level assuming a logarithmic velocity profile in the near-bed layer. This yields

$$u_* = \frac{\kappa u_b}{\ln \left(\frac{0.05h}{z_0} \right)} \dots \dots \dots (17)$$

in which u_b = flow velocity computed at $z = 0.05h$ above the mean bed level (Eq. 7).

Computation Procedure.—The complete set of Eqs. 9, 13, and 14 of

the profile-model is now defined and can be solved to determine the A_1 , t , and u_h variables. Substitution of these variables in Eq. 7 yields the velocity profile at each location. The input data are: discharge (Q), width (b), depth (h), effective roughness (k_s), Von Karman constant (κ), and the surface velocity at the inlet ($u_{h,0}$).

Calibration and Verification.—Eq. 14 has been calibrated by using velocity profiles measured in trenches situated perpendicular to the flow direction (4,18). The experiments were carried out in a flume (length = 17 m, width = 0.5 m, and depth = 0.7 m) of the Delft Hydraulics Laboratory. A Laser Doppler Velocity meter was used to measure the velocity profiles. The data of seven experiments with various trench geometries and hydraulic conditions were selected for calibration. The bottom slopes of the trench were in the range between 1:2 and 1:8, the Froude numbers were in the range from 0.1–0.3 and the bed roughness was in the range from 0.006–0.02 m.

Based on fitting of measured and computed velocity profiles, the α_1 and α_2 coefficients were determined and implemented in the SUTRENCH model (18). The α_3 coefficient represents the adjustment of the water surface velocity to lateral (width) variations. Since experimental data were not available, the α_3 coefficient could not yet be calibrated. Therefore, an expression is applied that yields a gradual adjustment of the surface velocity. Fig. 3 shows computed and measured velocity profiles for one of the calibration experiments. The width is constant ($db/dx = 0$). The bottom slopes of the trench are 1:4, which is rather steep. The depth-averaged approach velocity is 0.4 m/s. The bed roughness is $k_s = 0.02$ m. The agreement between measured and computed u -velocity profiles is reasonably good in the converging flow section, but less good

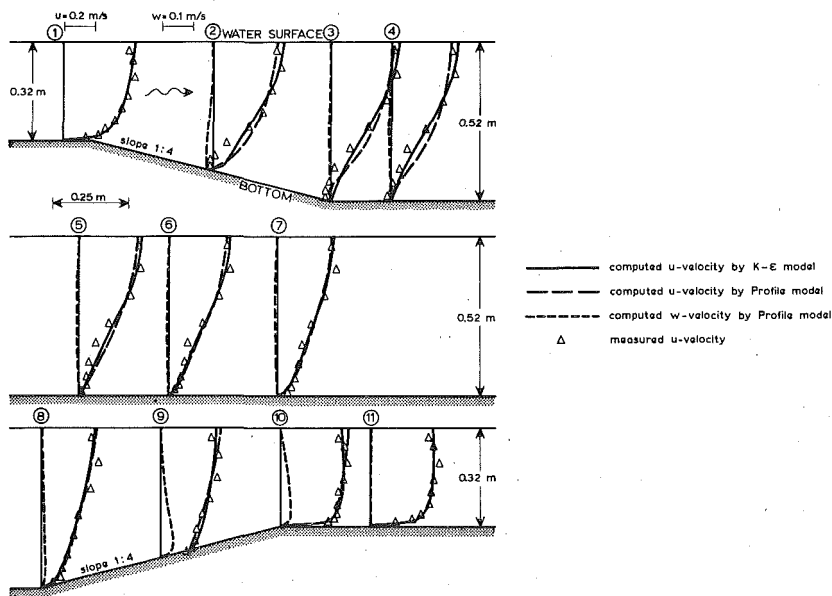


FIG. 3.—Computed and Measured Velocity Profiles

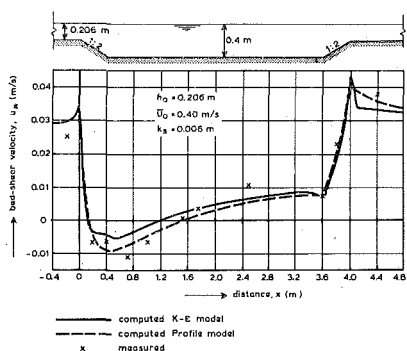


FIG. 4.—Computed and Measured Bed-Shear Velocities

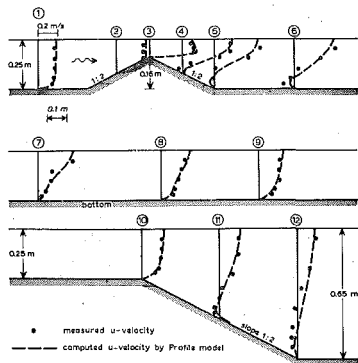


FIG. 5.—Computed and Measured Velocity Profiles

in the diverging flow section. The w velocities were not measured.

For comparison the results of the sophisticated $K-\epsilon$ model as presented by Alfrink and Van Rijn (1) are also shown. The results of the Profile model and the $K-\epsilon$ model show similar deviations compared with the measured values. Finally, note that the flow was not fully two-dimensional, because of the relatively small width-depth ratio of the flow. This is indicated by the unit width discharge in the centerline of the flume, which is relatively small in the diverging flow section compared with that in the inlet section.

Fig. 4 shows computed and measured bed-shear velocities for a trench with side slopes of 1:2.

The measured bed-shear velocities were derived from the velocities measured at $z = 0.02$ m above the bed by substituting these latter values in the logarithmic velocity distribution for hydraulic rough flow [$u = (u_*/\kappa) \ln(30z/k_s)$]. According to the law of the wall, the logarithmic velocity distribution is valid for the near-bed region ($z < 0.1h$). The Von Karman constant is assumed to be 0.4. Fig. 5 shows the performance of the Profile model for an experiment (in a flume) that has *not* been used in the calibration procedure of Eq. 14. Therefore, these results can be considered as an independent verification of the Profile model. The flow conditions are rather complicated showing the flow over a dam followed by a trench. The width is constant. The depth-averaged approach velocity is 0.185 m/s. The effective bed roughness is $k_s = 0.01$ m. The bottom slopes of the dam and trench are 1:2.

As can be observed, the agreement of the computed and measured velocity profiles is rather good. It may be noted that the inertial effects at the top of the dam causing a negative velocity gradient near the water surface are also represented.

As regards verification for field conditions, only some velocity measurements in the middle of a pipeline trench in a wide estuary (western Scheldt) in the Netherlands were available to verify the Profile method. Comparison of measured and computed velocity profiles at that location showed reasonable agreement (18). More extensive verification for field conditions is necessary to investigate whether the Profile model is a

powerful method for engineering practice. An advantage is the low computer costs (factor 100 lower than for the $K-\epsilon$ model), which is important because the computation costs of the fluid velocities is a major part of the total costs of the sediment transport model. Another advantage of the Profile model is the application of analytical expressions. A disadvantage is the validity range of the calibration coefficients. At present stage of research the Profile model is calibrated to represent the velocity profiles in a flow across (trapezoidal) channels and trenches. For other conditions the Profile model should be checked or recalibrated by fitting of measured and computed velocity profiles. When measurements are available, the calibration of Eq. 14 is easy and straightforward.

FLUID AND SEDIMENT MIXING COEFFICIENT

General Approach.—At present stage of research the best approach to compute the fluid mixing (or eddy viscosity) coefficient for complicated flow conditions is the application of the sophisticated $K-\epsilon$ model. has been shown that the $K-\epsilon$ model yields good results for the velocity profiles (1). Therefore, it is assumed that the underlying variables such as the mixing coefficients, ϵ_f , also represent realistic values. However, the application of the $K-\epsilon$ model is not very attractive for routine long-term computations because of excessive computer costs. For that reason, the simple profile method has also been used to represent the fluid mixing coefficient distribution. The Profile model for the fluid mixing coefficients has been calibrated by using fluid mixing coefficients computed by the sophisticated $K-\epsilon$ model for a wide range of conditions. Calibration using experimentally determined fluid mixing coefficients [$\epsilon_f = \tau/(\rho du/dx)$] was not possible, because accurate shear-stress, τ , measurements were not available. The Profile model for the mixing coefficient will now be described.

Vertical Distribution of Fluid Mixing Coefficients.—In the vertical direction a parabolic-constant profile is used, which means a constant (maximum) value in the upper half of the depth and a parabolic distribution in the lower half of the depth. This vertical distribution, introduced by Kerssens (8) and shown in Fig. 6, reads as

$$\epsilon_f = \epsilon_{f,\max} - \epsilon_{f,\max} \left(1 - \frac{2z}{h}\right)^2 \quad \text{for } \frac{z}{h} < 0.5 \dots \dots \dots (18a)$$

$$\epsilon_f = \epsilon_{f,\max} \quad \text{for } \frac{z}{h} \geq 0.5 \dots \dots \dots (18b)$$

The reason for applying a constant mixing coefficient in the upper half of the flow depth is the experimental work of Coleman (2) showing almost constant mixing coefficients in the upper half of the flow. It also yields a finite concentration at the water surface which is realistic. It is realized that a constant mixing coefficient is not correct in relation to the physics of the velocity profiles. However, the proposed parabolic-con-

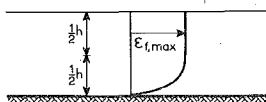


FIG. 6.—Vertical Distribution of Mixing Coefficient

stant mixing coefficient distribution is only used for (an optimal) computation of the sediment concentration profiles.

Longitudinal Distribution of Fluid Mixing Coefficient.—In longitudinal direction the variation of the mixing coefficient is effectuated by varying the $\epsilon_{f,max}$ value by use of a simple first order differential equation, as follows:

$$\frac{d}{dx}(\epsilon_{f,max}) = \left[\frac{\alpha_4}{h} (\epsilon_{f,max,e} - \epsilon_{f,max}) - \alpha_5 h \frac{d}{dx} (u_h - \bar{u}) \right] e^{-15dh/dx} \dots\dots\dots (19)$$

in which $\epsilon_{f,max,e} = 0.25 \kappa u_{*,e} h$ = maximum fluid mixing coefficient for equilibrium conditions; $u_{*,e} = (g^{0.5}/C) \bar{u}$ = equilibrium bed-shear velocity; \bar{u} = cross section averaged flow velocity; C = overall Chézy coefficient; and α_4 and α_5 = coefficients.

Eq. 19 represents the two most important processes influencing the longitudinal variation of the mixing coefficient: (1) The decrease of the $\epsilon_{f,max}$ value towards its equilibrium value (first term on right-hand side); and (2) the increase of the $\epsilon_{f,max}$ value after a change of the shape of the velocity profile (second term on right-hand side). The exponential term is a stabilizing term acting at steep sloping bottoms.

Calibration.—The α_4 and α_5 coefficients were determined by calibrating with computation results of the sophisticated $K-\epsilon$ model for various conditions concerning the flow in trenches (18). Fig. 7 shows calibration results for two flow situations.

Generally, the values in the upper half of the depth computed by the Profile model are larger than those computed by the $K-\epsilon$ model. This is not surprising because the values computed by the $K-\epsilon$ model are based on the specification of a parabolic mixing coefficient distribution at the inlet section (Fig. 7). Although the values in the upper layers computed by the Profile model are larger than those computed by the $K-\epsilon$ model, the effect of these discrepancies on the concentration profiles is rather small, as shown later on (Fig. 12). This can also be demonstrated by

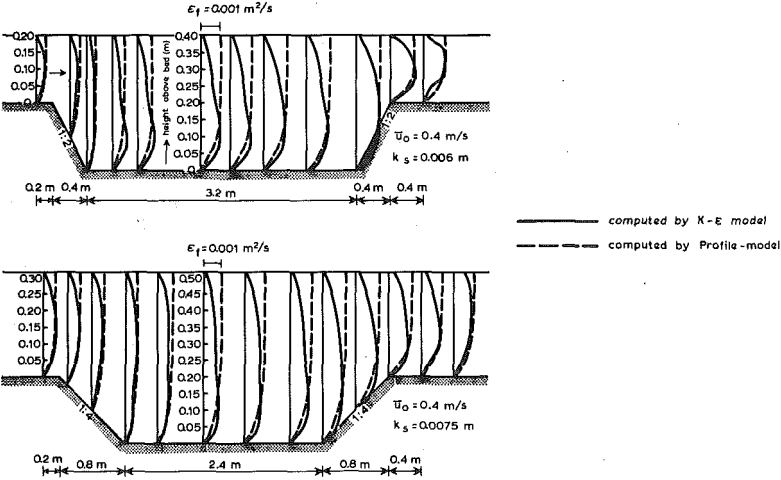


FIG. 7.—Computed Fluid Mixing Coefficients

comparing equilibrium concentration profiles based on a parabolic and a parabolic-constant distribution (19). A constant mixing coefficient in the upper half of the depth only yields significant larger concentrations in the near-surface layer ($z > 0.9 h$), where the concentrations based on a parabolic mixing coefficient reduce to a zero value at the water surface. More important are the values of the mixing coefficient in the near-bed region, especially when the erosion process dominates (converging flow). As can be observed, the $K-\epsilon$ model yields larger mixing coefficients in the near-bed region. This results in a more uniform sediment concentration profile and hence a somewhat larger depth-integrated suspended load, as will be shown later on in this paper (Fig. 12).

Sediment Mixing Coefficient.—The sediment mixing coefficient, ϵ_s , is related to the fluid mixing coefficient (ϵ_f) by

$$\epsilon_s = \beta \phi \epsilon_f \dots \dots \dots (20)$$

The β factor represents the difference in the mixing of a fluid particle (or small coherent fluid structure) and a discrete sediment particle. The β factor is assumed to be constant over the depth. Based on the experimental data of Coleman (2), the β factor was found to be (by the present writer) in the range of 1–3, depending on the ratio of the particle fall velocity and bed-shear velocity (14,17). The ϕ factor expresses the damping of the turbulence by the sediment particles resulting in a reduction of the fluid mixing coefficient. This effect was studied by Van Rijn (14,15,17). For concentrations smaller than about 10,000 ppm, the influence of the ϕ factor is relatively small and may, therefore, be neglected for most practical cases ($\phi = 1$).

EQUILIBRIUM CONCENTRATION PROFILE

For uniform or equilibrium conditions ($du/dx = 0$, $dc/dx = 0$), Eqs. 2, 18, and 20 yield the following equilibrium concentration profile:

$$\frac{c}{c_a} = \left[\frac{(a)(h-z)}{(z)(h-a)} \right]^Z \quad \text{for } z < 0.5 h \dots \dots \dots (21a)$$

$$\frac{c}{c_a} = \left[\frac{a}{h-a} \right]^Z [e]^{-4Z(z/h-0.5)} \quad \text{for } z \geq 0.5 h \dots \dots \dots (21b)$$

in which c_a = reference concentration at a small height a above the mean bed level; and $Z = w_s/(\beta \kappa u_{*,e})$ = suspension number.

BOUNDARY CONDITIONS AND INPUT PARAMETERS

Flow Domain.—The following specifications are required: (1) Initial bed level profiles, $z_b = f(x, t = 0)$; (2) water depth, $h = f(x, t = 0)$; (3) flow width, $b = f(x, t = 0)$; (4) particle fall velocity, w_s ; (5) effective bed roughness, k_s ; (6) bed material sizes, D_{50} and D_{90} ; and (7) β factor, β . The water surface is assumed to be horizontal. Variations due to acceleration and deceleration effects are neglected. This restricts the model to small-scale problems.

Inlet Boundary.—The following specifications are required: (1) Discharge, Q ; (2) flow velocity distribution, $u = f(z)$; (3) mixing coefficient distribution, $\epsilon_f = f(z)$; and (4) sediment concentration distribution, $c = f(z)$. Special cases are an equilibrium concentration profile or a zero-concentration profile (no initial load). Preferably, a measured concentration

profile should be used at $x = 0$. The inlet boundary should be selected at a location where no or minor morphological changes are to be expected.

Outlet Boundary.—The location of the outlet boundary should be far away from the area of interest. As the water surface is assumed to be horizontal, no additional specification of the local water depth is required.

Water Surface.—The net vertical sediment transport is assumed to be zero, resulting in

$$\left[w_s c + \epsilon_s \frac{\partial c}{\partial z} \right] = 0 \dots \dots \dots (22)$$

Bed Boundary.—The following conditions are used: (1) Flow velocity, $w = 0$ at $z = z_b + z_0$; and (2) sediment, bed concentration c_a at $z = z_b + a$, or upward sediment flux $E_a = (-\epsilon_s \partial c / \partial z)_a$ at $z = z_b + a$. Two options for the sediment input at the bed boundary are available in the SU-TRENCH model. The bed concentration, c_a , or the upward sediment flux, E_a , can be specified by known functions that relate both variables to local near-bed hydraulic and sediment parameters.

When the flow is varying rapidly (steep bottom slopes), the application of a bed-concentration type of boundary condition may result in a positive concentration gradient near the bed ($\partial c_a / \partial z > 0$) at a certain location (x_i). This is physically not realistic for a movable bed situation. In that case the concentration at that location (x_i) is recomputed using a zero-bed concentration gradient ($\partial c_a / \partial z = 0$) as bed-boundary condition. Finally, it is noted that the bed-boundary condition is specified at a small height (say half the bed-form height) above the mean bed level. This approach is attractive because in that case the bed concentration or sediment flux may be represented by its equilibrium value assuming that there is an almost instantaneous adjustment to equilibrium conditions close to the bed. Detailed experimental research has shown that these assumptions are reasonable (6).

Bed Concentration Function.—Based on theoretical and experimental research, the writer has proposed a simple deterministic function for equilibrium conditions that is valid for sand particles in the range 100–500 μm (14,17). This function reads

$$c_{a,e} = 0.015 \frac{D_{50} T^{1.5}}{D_*^{0.3}} \dots \dots \dots (23)$$

in which $T = (\bar{\tau}'_b - \bar{\tau}_{b,cr}) / \bar{\tau}_{b,cr}$ = bed shear-stress parameter; $D_* = D_{50}[(s - 1)g/\nu^2]^{1/3}$ = particle parameter; D_{50} = median particle size of bed material; $s = \rho_s/\rho$ = specific density; ρ_s = sediment density; ρ = fluid density; $\bar{\tau}'_b = \mu \bar{\tau}_b$ = effective bed-shear stress; $\bar{\tau}_b$ = overall bed-shear stress; $\mu = (C/C')^2$ = bed form or efficiency factor; $C' = 18 \log(12h/3D_{90})$ = Chézy coefficient related to grains; $C = 18 \log(12h/k_s)$ = overall Chézy coefficient; $\bar{\tau}_{b,cr}$ = critical bed-shear stress according to Shields; and ν = kinematic viscosity coefficient.

Eq. 23 specifies a dimensionless concentration. Multiplying by $\rho_s 10^3$ yields a value in milligrams per liter.

In case of complicated flow conditions where flow separation and flow reversal may occur, a deterministic approach as expressed by Eq. 23 can-

not be used because the deterministic approach yields a zero-bed concentration ($c_a = 0$) at locations where the time-averaged bed-shear stress approaches to zero (separation and reattachment points, Fig. 4). This is not realistic in a physical sense, because at those locations the turbulent fluctuations are large and are likely to cause a relatively large sediment pickup. Therefore, a new (stochastic) approach is introduced to represent the influence of the turbulent fluctuations by using the standard deviation of the mean bed-shear stress. Applying this latter approach, the bed concentration can be expressed as (18)

$$c_{a,e} = 0.03 \frac{D_{50}}{a} \frac{\overline{T}^{1.5}}{D_*^{0.3}} \dots \dots \dots (24a)$$

in which

$$\overline{T}^{1.5} = \frac{1}{(2\pi)^{0.5}} \left[\left(\frac{\sigma'}{\tau_{b,cr,1}} \right)^{1.5} |J_1| + \left(\frac{\sigma'}{\tau_{b,cr,2}} \right)^{1.5} |J_2| \right] = \text{stochastic shear} \dots (24b)$$

stress parameter; σ' = standard deviation of effective bed-shear stress; $\tau_{b,cr,1}$ = instantaneous critical bed-shear stress in local flow direction; $\tau_{b,cr,2}$ = instantaneous critical bed-shear stress against local flow direction; and J_1, J_2 = integrals representing the pickup action of the bed-shear stress (18).

The stochastic shear stress parameter shows absolute values of the J_1 and J_2 integrals because the pickup of bed material is not related to a specific direction; positive (in flow direction) as well as negative (against flow direction) bed-shear stresses can contribute to the sediment pickup process. The critical bed-shear stresses are related to the Shield values. Additional gravity effects for particles resting on a sloping bottom are taken into account (18). The standard deviation σ' , is related to the mean bed-shear stress at the inlet, $\sigma' = 0.4 \bar{\tau}_{b,0}$, which means a constant σ' parameter in the computation domain. The influence of this parameter on the suspended load transport is shown later on in this paper. Further experimental research is necessary to get more information of the turbulent fluctuations near the bed.

Upward Sediment Flux Function.—For equilibrium conditions it follows that

$$E_{a,e} = - \left(\epsilon_s \frac{\partial c}{\partial z} \right)_a = w_s c_{a,e} \dots \dots \dots (25)$$

Substitution of Eq. 24 in Eq. 25 yields

$$E_{a,e} = -0.03 w_s \frac{D_{50}}{a} \frac{\overline{T}^{1.5}}{D_*^{0.3}} \dots \dots \dots (26)$$

Application of Eq. 25 implies that at each location, x_i , the equilibrium sediment flux is specified. This type of approach was also used by O'Connor (9).

BED LEVEL CHANGES

Sediment Continuity Equation.—Once the sediment concentration field is known, the cross-section integrated sediment transport can be computed. After that the bed level changes are computed from the cross section integrated sediment continuity equation, as follows:

$$\frac{\partial}{\partial t} (bz_b) + \frac{1}{\rho_s(1-p)} \frac{\partial}{\partial x} (S_s + S_b) = 0 \dots \dots \dots (27)$$

in which z_b = bed level with respect to a horizontal datum; t = time; p = porosity factor of bed material; S_b = cross section integrated bed-load; S_s = cross section integrated suspended load.

Suspended Load Transport.—The suspended load transport is based on the computed velocity, u , and concentration, c , profiles as follows:

$$S_s = b \int_{z_b+a}^{z_b+h} ucdz \dots \dots \dots (28)$$

Bed Load Transport.—The movement of sediment particles below the bed-boundary level ($z < a$) is represented as bed-load transport using a simple formula. For uniform flow conditions the writer has proposed the following bed-load formula (13,14,16):

$$S_b = 0.053 b [(s-1)g]^{0.5} D_{50}^{1.5} \frac{\overline{T}^{2.1}}{D_*^{0.3}} \dots \dots \dots (29)$$

For nonuniform flow conditions where flow separation and reversal may occur, a stochastic approach is essential. Therefore, Eq. 29 has been modified to

$$S_b = 0.1 b [(s-1)g]^{0.5} D_{50}^{1.5} \frac{\overline{T}^{2.1}}{D_*^{0.3}} \dots \dots \dots (30a)$$

$$\text{in which } \overline{T}^{2.1} = \frac{1}{(2\pi)^{0.5}} \left[\left(\frac{\sigma'}{\tau_{b,cr,1}} \right)^{2.1} J_3 + \left(\frac{\sigma'}{\tau_{b,cr,2}} \right)^{2.1} J_4 \right]$$

= stochastic shear stress parameter. (30b)

J_3 and J_4 are integrals (18). The J_4 integral has a negative sign because it represents the movement of bed-load particles against the flow direction due to negative velocity fluctuations.

NUMERICAL SOLUTION METHODS AND ACCURACY

Sediment Concentrations.—To solve Eq. 3, a finite-element method based on weighted residuals according to the (modified) Galerkin-method is used (18,20).

The continuous solution (two-dimensional) domain is divided into a system of quadrangular elements. The vertical dimensions of the elements are relatively small close to the bed to provide a greater resolution in the zone where large velocity and concentration gradients exist. Between the nodes of the elements the unknown variable is represented by a linear function. Then, for each element the coefficients corresponding to the unknown variable at each node are determined. Finally, the (tridiagonal) coefficients matrix for the complete solution domain is determined, from which the coefficients can be found.

In the vertical direction a number of 10–15 nodal points is sufficiently accurate for sandy bed conditions (18). For silty conditions the number of nodal points in the vertical direction may be reduced to about 5. The velocity profiles have no influence on the number of nodal points because they are computed analytically (Profile model).

The accuracy of the finite-element method is shown for the classical problem of the adjustment of concentration profiles in a horizontally

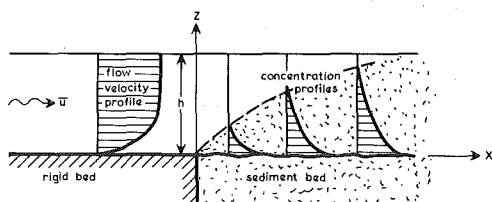


FIG. 8.—Adjustment of Concentration Profiles in Uniform Flow

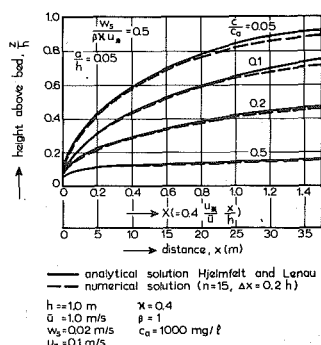


FIG. 9.—Numerically and Analytically Computed Concentrations

uniform flow which is initially ($x = 0$) free of sediment, as shown in Fig. 8.

Hjermfelt and Lenau (7) presented an analytical solution of Eq. 3 for a constant width assuming a parabolic mixing coefficient, a constant flow velocity in horizontal and vertical direction, $u = \bar{u}$, and a constant bed concentration in longitudinal direction.

Fig. 9 shows the analytical and the numerical solution for a specific case ($w_s / \beta \kappa u_* = 0.5$). The numerical method is based on 15 nodal points in vertical direction and a longitudinal step size (Δx) equal to 0.2 times the flow depth. The bed concentration is specified at $a = 0.05 h$. As can be observed, the numerical inaccuracy increases towards the water surface which is caused by the variable element size in vertical direction yielding relatively large element sizes near the water surface. The maximum error is about 10% applying 15 nodal points in the vertical direction, which is quite acceptable for engineering practice. The errors can be reduced by applying more nodal points in the vertical direction (at the expense of computation time). For example, the application of 25 nodal points results in a maximum error of 3%.

Bed Level Changes.—To compute the new bed level at time $t + \Delta t$ from the known bed level at time t , Eq. 27 is solved by using a conservative LAX scheme (18). This method, which is simple and straightforward, causes however some numerical smoothing (inaccuracy). To evaluate this latter effect, the LAX method was compared with a higher order predictor-corrector method (18,21). Long-term bed level computations using both methods showed differences less than 10%. Based on these results, the conservative LAX scheme is assumed to be sufficiently accurate for engineering practice.

SENSITIVITY ANALYSIS OF CONTROLLING PARAMETERS

Influence of Incoming Sediment Transport.—Generally, the inaccuracy of the (measured) sediment concentration profiles to be used as boundary conditions at the inlet ($x = 0$) is rather large. Variations of a factor 2 are commonly observed values. Fig. 10 shows the influence of the incoming suspended load on the computed sedimentation in a trench perpendicular to the flow direction (tidal flow). The influence appears to be rather large.

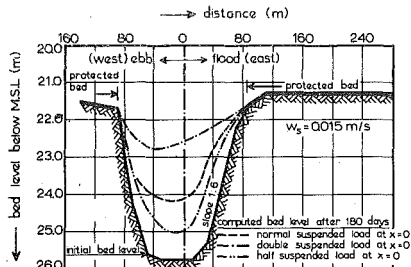


FIG. 10.—Influence of Incoming Suspended Load

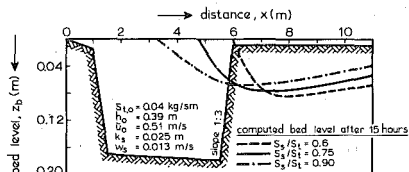


FIG. 11.—Influence of Ratio of Incoming Suspended Load to Total Load

Fig. 11 shows the influence of the ratio of the incoming suspended load, S_s to the total load, $S_t = S_s + S_b$, for an unidirectional flow. The total load is 0.04 kg/sm. A relatively large suspended load yields the least rapid migration of the upstream side slope. These results stress the importance of accurate measurements of the incoming sediment transport.

Influence of Particle Fall Velocity.—Usually, the representative particle fall velocity is determined from suspended sediment samples using laboratory or in situ analysis methods. For sandy bed conditions with a small gradation coefficient (say, $\sigma_s = 0.5 D_{84}/D_{50} + 0.5 D_{50}/D_{16} \approx 2$) the overall inaccuracy of the representative particle fall velocity may be as large as 25%.

Test computations show an inaccuracy of the total sedimentation rate in a trench of about 25% by varying the fall velocity with 25% ($w_s/u_* \approx 0.25$). When there are no measurements available, the fall velocity has to be estimated. This may lead to a considerably larger inaccuracy. This stresses the importance of detailed field measurements.

Influence of Mixing Coefficient.—The fluid mixing coefficients are computed by applying the Profile model, which has been calibrated by computation results of the sophisticated $K-\epsilon$ model. Fig. 7 shows results of the Profile and $K-\epsilon$ model for the same conditions. Considerable deviations can be observed in the upper half of the depth. To investigate

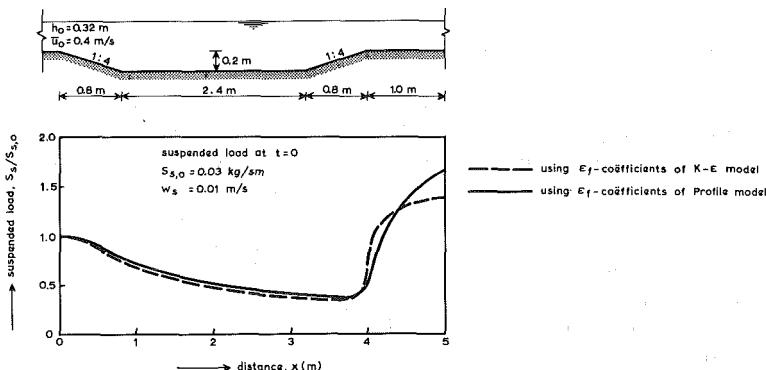


FIG. 12.—Influence of Mixing Coefficients

the effects of these deviations on the computed concentrations and the suspended load, the convection-diffusion equation (Eq. 3) has been solved using the mixing coefficients computed by both models.

Fig. 12 shows the computed suspended load for a trench (side slopes of 1:4) situated perpendicular to the flow. The sediment input at the bed is specified by using the upward sediment-flux function (E_a method). As it can be observed, the influence of variations of the mixing coefficients is negligibly small in the downsloping and middle section of the trench, and is mainly caused by the dominating effect of the settling process. In the upsloping section of the trench the mixing coefficients of the $K-\epsilon$ model yield the largest increase of the suspended load. This is caused by the relatively large values of the mixing coefficients in the lower half of the depth (Fig. 7).

Fig. 12 shows a maximum error of about 30% for a relatively steep bottom slope of 1:4, which is not very large considering the complicated nature of the erosion process. Generally, the errors will be less because of the presence of less steep slopes.

Influence of Bed Roughness.—The bed roughness, k_s , is an important parameter because it influences the velocity profile, the concentration profile and the sediment pickup process. In the present approach the influence of the k_s parameter on the pickup process is relatively small because the pickup process is related to the grain shear stress, $\bar{\tau}_b' = \mu \bar{\tau}_b$. A large k_s parameter yields a large $\bar{\tau}_b$ but a small μ factor (Eq. 23). The overall effect is small. Usually, the k_s parameter is evaluated from measured velocity profiles in the near-bed region. The inaccuracy of this method may be rather large (say, 100%). Therefore, the k_s parameter was varied by a factor 2 in the test computations for the sedimentation in a trench. The influence of the variation of the k_s parameter on the overall morphological changes was rather small ($\pm 20\%$).

It should be noted, however, that the incoming sediment transport was kept constant. This is realistic when measurements are available. If there are no measurements and the incoming sediment load has to be estimated, large errors may be introduced because the k_s parameter can have a large effect on the magnitude of the incoming sediment load, depending on the applied sediment transport formula. This, again, stresses the importance of measurements to specify the boundary conditions.

Influence of Reference Level.—Usually, the reference level at which the bed-boundary condition is specified, is chosen to be close to the mean bed (say, $a \approx 0.05 h$). For reasons of accuracy the reference level should not be smaller than $a = 0.01 h$ (14,17). Computations using reference levels in the range $a/h = 0.01 - 0.04$ showed a negligibly small effect on the long-term morphological changes for a trench (perpendicular to the flow).

Influence of Bed-Boundary Condition.—Two options are available: a specified bed concentration or a specified upward sediment flux. Fig. 13 shows the influence of these two types of conditions on the computed suspended load and bed levels after 15 hours for a trench. In the middle section of the trench, where the settling process dominates, the influence of the bed-boundary condition on the initial suspended load is negligibly small. In the upsloping section of the trench the flux type of boundary condition yields a more gradual adjustment of the initial sus-

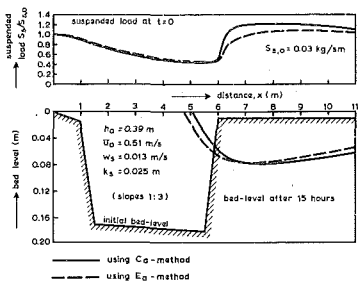


FIG. 13.—Influence of Bed-Boundary Condition

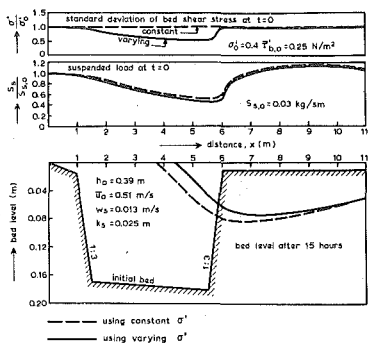


FIG. 14.—Influence of Standard Deviation of Effective Bed-Shear Stress

pendent load. The long-term effects (after 15 hours) are relatively small.

Influence of Standard Deviation of Bed-Shear Stress.—The computation of the bed-boundary condition by Eq. 24 or 25 implies the specification of the standard deviation of the effective bed-shear stress, σ' . For strongly nonuniform conditions such as the flow in a steep-sided trench, the σ' parameter is not known. To investigate the influence of the σ' parameter, the suspended load and the long-term bed levels in a trench were computed using a constant σ' and a varying σ' , as shown is Fig. 14. A varying σ' parameter implies a gradual decrease from $\sigma' = \sigma'_0$ at the inlet to $\sigma' = 0.5 \sigma'_0$ at the toe of the downstream side slope, assuming that the σ' value will be smaller in the channel where the velocities are reduced. A rather large reduction of the σ' value has been assumed to identify the influence of the σ' parameter as clearly as possible. A constant σ' parameter yields the largest sediment input at the bed and hence the largest suspended load. The computed bed level (after 15 hours) shows relatively small long-term effects. For most practical purposes a constant σ' parameter may be used.

VERIFICATION ANALYSIS

Adjustment of Sand Concentrations.—The adjustment of sediment concentration profiles in a steady, uniform flow, which is initially free of sediment, is studied (as shown in Fig. 8). Such an experiment was performed in a flume (length = 30 m, width = 0.5 m, depth = 0.7 m) of the Delft Hydraulics Laboratory (6). The water depth was 0.25 m. The mean velocity was 0.67 m/s. The bed material consisted of sand with $D_{50} = 230 \mu\text{m}$ and $D_{90} = 320 \mu\text{m}$. Based on suspended sediment samples, the representative particle size of the suspended sediment was found to be about $200 \mu\text{m}$, resulting in a fall velocity of about 0.022 m/s (water temperature of 9°C). Pitot-tubes were used to measure the velocity profile. Water samples were collected simultaneously in 5 profiles using 4 points in each profile. The measuring period was as short as possible to reduce the scouring depth downstream of the rigid bed to a minimum. The SUTRENCH model was used to simulate this experiment. At the inlet boundary ($x = 0$) a zero-concentration profile was specified. Since the objective of the simulation run is to represent the adjustment process and not to predict the equilibrium concentration profile at the end of

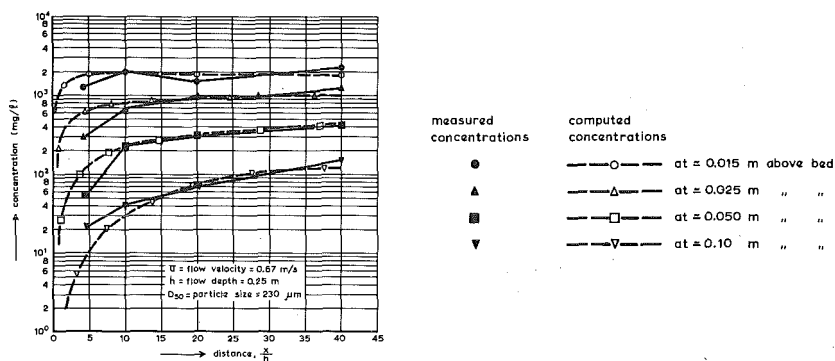


FIG. 15.—Computed and Measured Concentrations in Uniform Flow

channel, the bed-concentration and the β factor (Eq. 20) were fitted to obtain an optimal representation of the concentration profile measured at the end of the flume. This resulted in $c_a = 1,900$ mg/L at $a = 0.005$ m above the mean bed level and $\beta = 1.25$. The transition in bed roughness from the rigid flat bed to the movable bed forms has been taken into account by specifying $k_s = 0.0005$ m for the rigid flat bed and $k_s = 0.01$ m for the movable bed (bed-form height ≈ 0.015 m). The numerical parameters are $\Delta x = 0.2$ m and 10 grid points in vertical direction. Fig. 15 shows measured and computed concentrations as a function of space (x, z). The agreement is reasonably good with exception of the initial section ($x \leq 5h$), which is probably caused by the generation of a small scour hole with a depth of about 0.02 m in that section. As a result the local near-bed velocities were reduced somewhat resulting in a reduced pickup of bed material and smaller concentrations. The present computation results show somewhat better agreement with measured values than those of an earlier computation in which the transition in bed roughness was not represented (12).

Migration of Trench.—The SUTRENCH model was used to simulate the migration of a trench (perpendicular to flow), as measured in a flume (length = 30 m, depth = 0.7 m, width = 0.5 m) of the Delft Hydraulics Laboratory (5). Three tests were carried out with sand ($D_{50} = 160$ μm ; $D_{90} = 200$ μm) supplied at a rate of 0.04 kg/sm (= total load) to maintain equilibrium conditions (no scour or deposition) in the section upstream of the trench. The mean flow velocity and water depth at that section were $\bar{u}_0 = 0.51$ m/s and $h_0 = 0.39$ m during all tests. The trench dimensions were varied using initial side slopes of 1:3, 1:7, and 1:10. The velocities were measured by using an Ott-type propeller meter. The sand concentrations were determined by analyzing water samples collected in the centerline of the flume. Based on the measured velocity and concentration profiles in the upstream section, the equilibrium suspended load was computed to be about $s_s = 0.03$ kg/sm ($\pm 25\%$) resulting in a bed load $s_b = 0.01$ kg/sm ($\pm 25\%$). Based on the analysis of suspended sediment samples, the representative particle size of the suspended sediment was found to be about 130 μm resulting in a fall velocity of $w_s = 0.013$ m/s (water temperature = 15° C).

Based on the analysis of the velocity profiles, the effective roughness

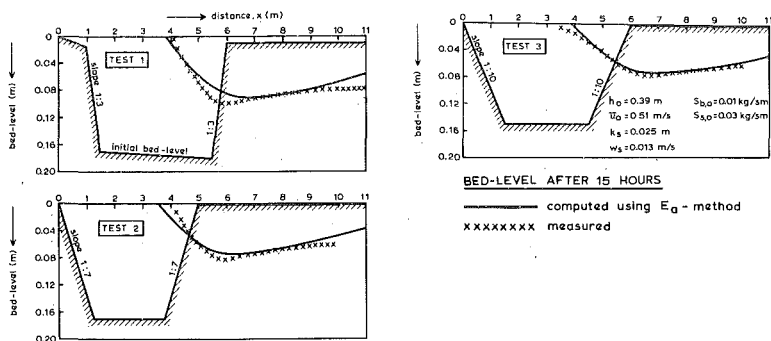


FIG. 16.—Computed and Measured Bed-Level Profiles

was found to be $k_s = 0.025$ m, which is a reasonable value compared with the observed bed-form heights in the range of 0.015–0.035 m.

Eq. 21 was used to respect the concentration profile at the inlet ($x = 0$). The β factor was determined by calibration yielding $\beta \approx 1$. The velocity profile at the inlet was assumed to be logarithmic. The maximum fluid mixing coefficient at $x = 0$ was computed to be $\epsilon_{f,\max,0} = 0.00155$ m²/s. The bed-boundary condition was applied at a level $a = 0.0125$ m using the sediment-flux method (E_a method, Eq. 26). The constant of Eq. 26 was adjusted somewhat to give a suspended load of $s_s = 0.03$ kg/sm at the inlet. The constant of the bed load formula (Eq. 30) was adjusted to give $s_b = 0.01$ kg/sm at the inlet ($x = 0$).

The numerical parameters are $\Delta x = 0.25$ m, 10 grid points in vertical direction and $\Delta t = 900$ s. The computed bed-level profiles after 15 hours are presented in Fig. 16 showing an extremely good agreement for all three trenches. Fig. 17 shows measured and computed velocity and sand concentration profiles at initial time ($t = 0$) for the trench with slopes 1:3.

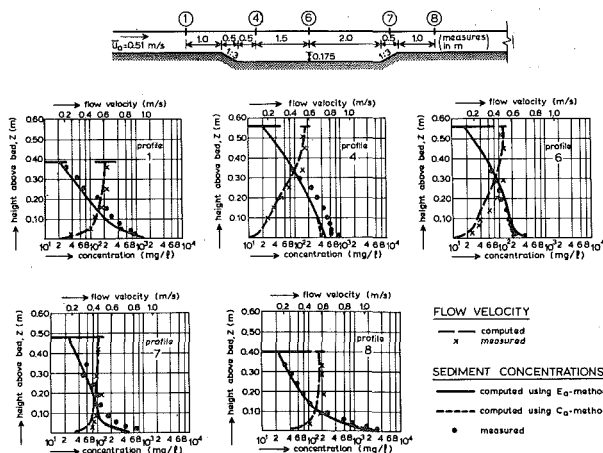


FIG. 17.—Computed and Measured Concentrations in Trench

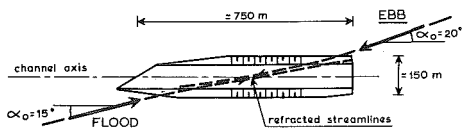


FIG. 18.—Trial Dredge Channel, Asan Bay, Korea

The measured velocities are systematically somewhat larger than the computed values, which is caused by the fact that the measurements were made in the centerline of the flume, while the computed values represent cross section averaged values. The computed concentrations show reasonably good agreement with the measured values, particularly in the middle section (profile 6). Both the c_a and E_a method have been used as bed-boundary condition.

As can be observed, the influence of the bed-boundary condition is relatively small. Only the near-bed concentrations are influenced showing variations upto a factor of 2. These near-bed effects do not seriously influence the depth-integrated suspended load.

Sedimentation and Erosion of Trial Dredge Channel near Korea.—In the summer of 1983, a trial dredge channel was made in the Asan Bay near Korea to obtain information of the sedimentation rates for a navigation channel. Physical and mathematical models were operated to determine the flow patterns near the trial dredge channel. The approach angle of the flood current was 15° and that of the ebb current was 20° , as shown in Fig. 18. Because of streamline refraction the angle between the current in the channel and the channel axis was reduced to about 10° for the flood as well as the ebb phase. Analysis of tidal data showed a semi-diurnal tide with a small diurnal inequality.

The mean tidal range was about 6 m. Maximum current velocities were in the range 0.6–1.2 m/s. The bed consisted of sand with $D_{50} \approx 200 \mu\text{m}$. Bed forms were present with a height of 0.25–0.5 m and a length of 25–50 m (echo soundings). The mean tidal cycle was schematized to 2 quasi-steady periods of 6 hours each. The characteristic current velocities were 0.78 m/s for the flood phase and 0.66 m/s for the ebb phase. The SUTRENCH model was applied to compute the sediment transport and morphological changes along the (refracted) streamlines. The depth-averaged velocities along the streamlines were determined from a two-dimensional horizontal model. These velocities were specified to the SUTRENCH model (by varying the width, b , along the trajet). At the inlet boundary an equilibrium concentration profile was assumed to be present, as described by Eq. 21. As bed-boundary condition the E_a method (Eq. 26) was used at a reference level of $a = 0.15$ m above the mean bed. The bed roughness was assumed to be $k_s = 0.15$ m. The representative particle size of the suspended sand was estimated to be equal to $0.75 D_{50, \text{bed}}$ resulting in a value of $150 \mu\text{m}$ (17) and a particle fall velocity of 0.016 m/s (water temperature of 20°C). The influence of the waves (in the range 0.25–0.5 m) on the sediment transport has been neglected. Fig. 19 shows measured and computed bed-level profiles after 100 days.

The agreement is rather good, particularly at the banks of the channel where erosion of bed material can be observed. In the middle of the channel there is also a small section with erosion. This effect was not

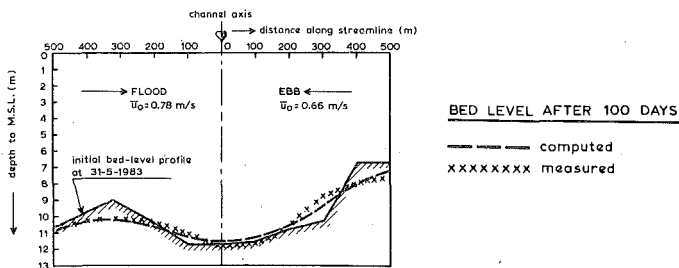


FIG. 19.—Computed and Measured Bed-Level Profiles, Asan Bay, Korea

predicted by the SUTRENCH model, probably because of an underprediction of the current velocity in that section of the channel.

CONCLUSIONS

The following conclusions are reached:

1. The proposed model for suspended sediment transport in nonuniform conditions yields reliable results in predicting the sediment concentrations, transport and bed-level changes in dredged channels, as shown by a verification analysis for unidirectional and tidal flow.
2. The Profile method applied to compute the fluid velocities and mixing coefficients can be a powerful method for engineering practice because of the application of analytical expressions and low computation costs. A disadvantage is the need for empirical data to calibrate the model.
3. The sediment input at the bed (boundary condition) in a nonuniform flow can be represented sufficiently accurately by specifying a bed concentration or an upward sediment flux. Stochastic functions are proposed to relate these variables to local bed-shear stress and sediment particle parameters.
4. Based on a sensitivity analysis, the most important controlling parameters are found to be: (1) The incoming bed and suspended load; and (2) the representative fall velocity of the suspended sediment particles. Variations (within reasonable ranges) of other hydraulic parameters did not seriously affect the predicted long-term bed-level changes. This is also valid for the type of bed-boundary condition and the applied reference level.

A two-dimensional mathematical model for suspended sediment transport in nonuniform flow conditions has been presented. This model has been developed as a tool for routine morphological computations in the daily engineering practice. For that purpose the fluid velocity and mixing coefficient distributions have been represented as simple as possible. This, inevitably, means a compromise between the representation of the physics of the flow and sediment transport, the overall accuracy of model and the computation costs.

The most sophisticated modeling of the sediment concentration profiles requires the application of the K - ϵ model. At present stage of computer power, however, this latter model is not attractive for routine morphological computations because of excessive computation costs. Therefore, a more simple model based on shape functions (profiles) to

represent the vertical distribution of the velocities and mixing coefficients, has been proposed. Disadvantages of this approach are the need for empirical data to calibrate the applied coefficients and a loss of accuracy because of a less sophisticated representation of the physics of the relevant processes. To justify the application of the simple Profile model, this latter model has been compared with the refined $K-\epsilon$ model showing good results for the fluid velocities but less accurate results for the mixing coefficients. Applying both models to compute the depth-integrated suspended load transport, a maximum relative error of about 30% was found for a steep-sided channel (Fig. 12). The magnitude of this deviation is considered to be reasonably small taking into account the complexity of the physics of the sediment transport process. The validity of the proposed approach is also shown by the simulation runs of the migrating (steep-sided) channel showing a quite good prediction of the long term bed level changes (Fig. 16).

Although the Profile model has been calibrated to represent a wide range of velocity profiles, more verification using field data is necessary to get a better understanding of the accuracy of the model. The application of the proposed model is essential for complicated flow conditions with strongly perturbed velocity profiles, provided that accurate boundary conditions are available. In the case of a flow over a gradually varying bottom topography, a more simple approach applying logarithmic velocity profiles at all locations can be used (18).

The presented sensitivity analysis has shown that the overall accuracy of the full sediment transport model is largely determined by the accuracy of the boundary conditions such as the suspended and bed load transport at the inlet boundary and the particle fall velocity. When accurate boundary conditions (field data) are missing, the application of the proposed model is not appropriate. In that case a less complicated approach should be used such as simple sediment transport relations or graphs. Finally, the importance of detailed field measurements to specify the boundary conditions is stressed, especially when an accurate morphological prediction is required.

APPENDIX.—REFERENCES

1. Alfrink, B. J., and Rijn, L. C., van, "Two-Equation Turbulence Model for Flow in Trenches," *Journal of Hydraulic Engineering*, ASCE, Vol. 109, No. 7, July, 1983, pp. 941–958.
2. Coleman, N. L., "Flume Studies of the Sediment Transfer Coefficient," *Water Resources Research*, Vol. 6, No. 3, 1970.
3. Coles, D., "The Law of the Wake in the Turbulent Boundary Layer," *Journal of Fluid Mechanics*, Vol. 1, 1965.
4. Delft Hydraulics Laboratory, "Semi-Empirical Model for the Flow in Dredged Trenches," *Report R 1267 III*, Delft, The Netherlands, 1980.
5. Delft Hydraulics Laboratory, "Computation of Siltation in Dredged Trenches: Mathematical Model," *Report R 1267 V*, Delft, The Netherlands, 1980.
6. Delft Hydraulics Laboratory, "Development of Sediment Concentration Profiles in a Steady Uniform Flow without Initial Sediment Load," *Report M.1531 II and III*, Delft, The Netherlands, 1981 and 1983.
7. Hjelmfelt, A. T., and Lenau, C. W., Non-Equilibrium Transport of Suspended Sediment, *Journal of the Hydraulic Division*, ASCE, HY 7, July, 1970, pp. 1567–1586.
8. Kerssens, P. J. M., Prins, A., and Rijn, L. C., van, "Model for Suspended

- Sediment Transport," *Journal of the Hydraulic Division*, ASCE, HY 5, May, 1979, pp. 461-476.
9. O'Connor, B. A., Siltation in Dredged Channels, Paper E2, Symposium on Dredged Technology, Univ. of Kent, Canterbury, England, 1975.
 10. Rodi, W., "Turbulence Models and their Application in Hydraulics," IAHR Section on Fundamentals, Delft, The Netherlands, 1980.
 11. Rijn, L. C., van, "Model for Sedimentation Predictions," 19th IAHR Congress, New Delhi, India, 1981.
 12. Rijn, L. C., van, "The Development of Concentration Profiles in a Steady Uniform Flow without Initial Sediment Load," IAHR Workshop on Particle Motion and Sediment Transport, Rapperswil, Switzerland, 1981.
 13. Rijn, L. C., van, "Computation of Bed Load Concentration and Bed Load Transport," *Report S 487 I*, Delft, The Netherlands, 1981.
 14. Rijn, L. C., van, "Computation of Bed Load and Suspended Load," *Report S 487 II*, Delft, The Netherlands, 1982.
 15. Rijn, L. C., van, "Sediment Transportation in Heavy Sediment Laden Flows," *International Symposium on River Sedimentation*, Nanjing, China, 1983.
 16. Rijn, L. C., van, "Sediment Transport, Part 1: Bed Load Transport," *Journal of Hydraulic Engineering*, ASCE, No. 10, Oct. 1984, pp. 1431-1456.
 17. Rijn, L. C., van, "Sediment Transport, Part 2: Suspended Load Transport," *Journal of Hydraulic Engineering*, No. 11, Nov., 1984, pp. 1613-1641.
 18. Rijn, L. C., van, "Two-Dimensional Vertical Mathematical Model for Suspended Sediment Transport by Currents and Waves," *Report S 488 IV*, Delft, The Netherlands, 1984.
 19. Rijn, L. C., van, "Mathematical Models for the Computation of Sediment Concentration Profiles in Steady Flow," Invited Lecture, Euromech Colloquium 192, Munich, West Germany, 1985.
 20. Vreugdenhil, C. B., "Numerical Solution of a Convection-Diffusion Equation Using Finite Elements," Note X 59, Delft, The Netherlands, 1982.
 21. Vreugdenhil, C. B., "Finite-Difference Methods for Bed Level Computation for an Unknown Migration Velocity," in Dutch, Note X 61, Delft, The Netherlands, 1982.